frontiers | Frontiers in Hematology

TYPE Original Research
PUBLISHED 18 April 2024
DOI 10.3389/frhem.2024.1356561

OPEN ACCESS

EDITED BY
Anna Rita Migliaccio,
Campus Bio-Medico University, Italy

REVIEWED BY
Ioanna Triviai,
Max Planck Institute for Molecular Genetics, Germany
Tayler Van Denakker,
Icahn School of Medicine at Mount Sinai, United States

*CORRESPONDENCE
Cecilia Carubbi
cecilia.carubbi@unipr.it
Elena Masselli
elena.masselli@unipr.it

†These authors have contributed equally to this work

RECEIVED 15 December 2023
ACCEPTED 13 March 2024
PUBLISHED 18 April 2024

CITATION
Pelagatti L, Pozzi G, Cortellazzi S, Mancini C, Martella E, Pagliaro L, Giaimo M, Roti G, Vitale M, Carubbi C and Masselli E (2024) Morphological, clinical, and molecular profiling of post-polycythemia vera accelerated/blast phase occurring with and without antecedent secondary myelofibrosis. *Front. Hematol.* 3:1356561.
doi: 10.3389/frhem.2024.1356561

Morphological, clinical, and molecular profiling of post-polycythemia vera accelerated/blast phase occurring with and without antecedent secondary myelofibrosis

Laura Pelagatti[1†], Giulia Pozzi[2†], Samuele Cortellazzi[2], Cristina Mancini[3], Eugenia Martella[3], Luca Pagliaro[1,4], Mariateresa Giaimo[1,4], Giovanni Roti[1,4], Marco Vitale[5], Cecilia Carubbi[2*] and Elena Masselli[1,2*]

[1]Hematology and Bone Marrow Transplant (BMT) Unit, Parma University Hospital (AOU-PR), Parma, Italy, [2]Anatomy Unit, Department of Medicine and Surgery (DiMeC), University of Parma, Parma, Italy, [3]Pathology Unit, Parma University Hospital (AOU-PR), Parma, Italy, [4]Translational Hematology and Chemogenomics (THEC), Department of Medicine and Surgery (DiMeC), University of Parma, Parma, Italy, [5]Faculty of Medicine and Surgery, University Vita-Salute San Raffaele, Milan, Italy

Introduction: Polycythemia vera (PV) is a *JAK2*-mutated myeloproliferative neoplasm (MPN) characterized by clonal erythrocytosis and an intrinsic risk of transformation into acute myeloid leukemia (AML), known as blast-phase (BP) disease, a condition typified by dismal prognosis. In PV, the evolution to BP generally occurs through an overt fibrotic progression, represented by the post-PV myelofibrotic (MF) stage. However, direct leukemic transformation from PV may also occur in up to ~50% of patients. In this study, we sought to shed light on the morphological, clinical, and molecular features that may differentiate BP arising from a direct transition from the PV stage (post-PV-BP) from those evolving through a diagnosis of post-PV myelofibrosis (post-PV-MF-BP).

Methods and results: We retrospectively analyzed a cohort of post-PV-BP (n=5) and post-PV-MF-BP (n=5). We found that BP arising from PV directly displayed significantly lower leukocyte count (median 2.93 × 10^9/L, range: 2.30–39.40 vs. median 41.05 × 10^9/L, range: 5.46–58.01; P=0.03), and spleen diameter (14.0 cm, range: 11.5–20.0 vs. 25.5 cm, range: 18–26; P=0.03) as compared to those experiencing an overt fibrotic stage. The most striking differences emerged from bone marrow (BM) morphological analysis: all post-PV-BP were characterized by significantly higher cellularity (median 70%, range: 60%–98% vs. 28%, range: 2%–41%, P=0.0245), lower degree of fibrosis (fibrosis grade 1 vs. fibrosis grade 3 in all cases, P=0.008) and dysplastic features involving all three lineages, most prominently the erythroid and megakaryocytic compartment. Next-generation sequencing (NGS) analysis revealed that post-PV-BP cases were enriched in mutations located in genes involved in DNA methylation such as *DNMT3A, IDH1/2,* and *TET2* (45% vs. 15%, P=0.038).

Discussion: With all the limits of the small number of patients for each cohort, our data suggest that BPs that arise directly from PV present a peculiar phenotype, consistent with the molecular signature of the disease, typified by mutations of genes occurring with a high frequency in Myelodysplastic Syndromes (MDS) and MDS/MPN. Further studies in larger cohorts are warranted to translate these observations into robust evidence that may advise therapeutic choices.

KEYWORDS

polycythemia vera, blast-phase, accelerated phase, bone marrow morphology, mutational profile

1 Introduction

Polycythemia vera (PV) is a *JAK2*-mutated myeloproliferative neoplasm (MPN) typified by clonal erythrocytosis. Along with primary myelofibrosis (PMF) and essential thrombocythemia (ET), PV belongs to the classic Philadelphia-negative MPN. PV can lead to significant morbidity and increased mortality, with patients experiencing a reduced quality of life, a high rate of vascular events, and the potential intrinsic risk of disease evolution. Mutations in *JAK2* Exon 12-15 encompass the vast majority (97%–98%) of PV mutational landscape (1). In addition, over 50% of patients harbor non-driver mutations in specific myeloid genes with the most frequent being *TET2* (18%), *ASXL1* (15%), and *SH2B3* (3%) (2).

Approximately 15% of patients with PV experience a fibrotic progression of their disease over time, termed post-PV myelofibrosis (post-PV-MF) (2) and about 3% evolve, over a period of 10 years, into accelerated (MPN-AP) and blast phase (MPN-BP) disease (3), operationally defined by 10% to 19% or ≥ 20% myeloid blasts in the peripheral blood or bone marrow, respectively (4). However, despite this formal classification, MPN patients with 5% or more circulating/marrow blasts can be on a spectrum that leads to MPN-BP, with similar poor survival rates (5).

Clinical and molecular risk factors for leukemic evolution have been identified by the Mayo-Florence study conducted on 410 patients with MPN-BP, with 97 patients whose condition progressed from an antecedent PV, either directly (46 patients) or through a post-PV-MF stage (51 patients). Hematological risk factors are leukocytosis ≥11 × 10^9/uL (Florence cohort) or ≥15 × 10^9/uL (Mayo cohort), older age (> 67 years, both cohorts), abnormal karyotype (Mayo cohort), presence of *IDH2* and *RUNX1* mutations (Mayo cohort), and *SRSF2* mutations (Florence cohort) (3).

On these bases, investigators generated a mutation-enhanced international prognostic system for chronic phase disease (MIPSS-PV), which included presence of adverse mutations (*SRSF2*) (two points); abnormal karyotype (one point); age >67 years (three points); and leukocyte count ≥15 × 10^9/uL (two points) (6). Additionally, it is well established that previous treatment with radiophosphorous, chlorambucil, or pipobroman increases the risk of leukemic transformation (3).

The evolution to AP and BP is an almost invariably fatal event in the course of PV (and MPN in general), with a median overall survival (OS) of 13 months for AP and 3–5 months for BP, due to disease aggressiveness and limited therapeutic options, especially for transplant ineligible patients (4). The lack of standardized treatment(s) mirrors our still fragmented understanding of the molecular mechanisms underlying the progression of an MPN to AP/BP. It is currently acknowledged that the acquisition of additional somatic mutations and epigenetic alterations in hematopoietic progenitor and stem cells play a pivotal role in leukemic transformation, accounting for the selection and expansion of the malignant clone on one side, and on the other side, the generation of a tumor supportive proinflammatory microenvironment. Two main models of leukemic transformation have been proposed: (i) the acquisition of additional mutations by the *JAK2/CALR/MPL*-positive clone (7) and (ii) the emergence and expansion of a leukemic clone distinct from the clone bearing an activating driver mutation, eventually overcoming the MPN *JAK2/CALR/MPL*-mutated clone (7). In the first setting, the most common genetic alteration is represented by *TP53* mutations, detected in approximately 15% of patients with *JAK2*V617F (showing cooperative activity) and 25% of patients with *CALR* mutations. In the second scenario, a decrease in variant allele frequency (VAF) or loss of pre-existing driver mutation is usually observed (4). In addition to these two scenarios, another possible mechanism has been suggested, focused on the timing of occurrence of mutations involving chromatin modifiers, spliceosome complex components, DNA methylation modifiers, tumor suppressors, and transcriptional regulators. These mutations are described as coexisting mutations since their presence within a clone can precede the acquisition of the driver mutation or can occur subsequently. Grabek et al. (8) suggested that specific coexisting mutations in the same driver-mutated clone may favor direct leukemic transformation while others may drive progression to myelofibrosis which in turn may evolve into AP/BP.

Independent from the molecular pathway leading to MPN-AP/BP, it is well established that the mutational profile and overall prognosis of acute myeloid leukemia (AML) resulting from an antecedent MPN remains distinct from that in *de novo* AML (2, 4, 9). Indeed, mutations in *FLT3* and *NPM1* are rarely seen in MPN-BP, while, in addition to driver mutations, frequently mutated genes are *ASXL1* (30%), *TET2* (25%), *SRSF2* (22%), *RUNX1* (20%), and *TP53* (17%). Moreover, 25% and 46% of patients, harbor mutations in 3 and ≥4 genes, respectively. *TP53* is the only individual mutation to correlate with shorter OS (9).

In PV, the evolution to MPN-AP/BP generally occurs through a fibrotic progression, represented by the secondary (post-PV) MF stage, whose diagnosis is codified by the IWG-MRT criteria (10). However, direct leukemic transformation from a florid disease (PV) to AP/BP may also occur. Data from the Mayo-AGIMM study indicate that cases of post-PV AP/BP without a documented MF phase range from 37% (AGIMM cohort) to 53% (Mayo cohort). Similar rates were found for post-ET BP (58% and 55% in the two cohorts, respectively) (3).

So far, studies have mainly focused on the comparison of the clinical and biological characteristics of MPN-AP/BP vs. *de novo* AML. Here, we analyzed the morphological, clinical, and molecular features of patients with post-PV AP/BP arising from a direct progression from PV to leukemic phase (overall, termed post-PV-BP), and compared them with those transitioning through a documented overt fibrotic stage (termed post-PV-MF-BP), documenting that post-PV-BP is characterized by unique features, distinct from post-PV-MF-BP.

2 Methods

The current study is a single-center descriptive retrospective review of 10 consecutive cases of AP/BP evolving from an antecedent PV, either directly, without a documented overt fibrotic progression (termed post-PV-BP, five patients, with two AP and three BP), or through a documented MF stage, i.e., diagnosis of post-PV-MF (termed post-PV-MF-BP, five patients, all BP), followed at the Hematology and BMT Unit of Parma University Hospital.

Demographic, clinical, and molecular data at the time of PV diagnosis and leukemic transformation were collected in a dedicated database after patient de-identification by univocal alphanumeric codes (Ethical Committee approval: protocol 6923, 17/02/2020). Diagnosis of PV, post-PV-MF, and AP/BP was determined according to the WHO/IWG-MRT criteria (10, 11).

Cytogenetic analysis was performed according to the International System for Human Cytogenetic Nomenclature criteria. High-risk karyotype included monosomal karyotype and single or multiple cytogenetic abnormalities of −7, inv(3)(q21.3q26.2)/t(3,3)(q21.3;q26.2), i(17)(q10)/-17/abn(17p) (3). NGS analysis for target myeloid genes was performed by Myeloid Solutions Panel (SOPHiA Genetics, Saint Sulpice, Switzerland). Alignment, base calling, and variant annotation were performed with SOPHiA DDM software and investigating available databases (such as NCBI, COSMIC, GNOMAD, CLINVAR, and ExAC). Pathogenic relevant mutations (category A and B) were characterized by a functional analysis through Hidden Markov Models (FATHMM) score >0.90, while genetic variants that have been flagged as an SNP in the Catalogue of Somatic Mutations In Cancer (COSMIC) database and/or reported as of undetermined significance/benign/likely benign in ClinVar database belonged to category C or D and had a low FATHMM score (<0.5).

Bone marrow biopsies were fixed in neutral buffered formalin, decalcified with ethylenediamine tetra-acetic acid and paraffin embedded for routine diagnostic purposes. Paraffin sections were used for hematoxylin-eosin staining and for reticulin staining. BM age-adjusted cellularity was evaluated according to the European Myelofibrosis Network (EUMNET) consensus (12), and the grading of BM fibrosis was assessed semi-quantitatively following the European consensus guidelines (12). BM sections were also immunostained by using antibodies against CD34 (clone QBend/10), CD61 (clone2f2), CD71 (clone MRQ-48), and myeloperoxidase (polyclonal antibody) (Ventana-Roche, Basilea, Switzerland). Immunostaining was carried out with polymeric system Ultraview 3,3′-diaminobenzidine DAB IHC Detection Kit (Ventana-Roche, Basilea, Switzerland), on a BenchMark ULTRA IHC/ISH instrument (Roche, Basilea, Switzerland), in accordance with the manufacturer's protocols. Images were captured and analyzed by an Olympus DP22 digital camera (Ventana-Roche, Basilea, Switzerland).

Immunophenotyping was performed using BD FACSLyric™ Flow Cytometer (BD™ Biosciences, Franklin Lakes, NJ, USA). Peripheral blood samples (3–5 mL in EDTA tubes) were processed with lyse and wash protocol. After labeling with antiCD45-APC-H7, antiCD34-PerCP-Cy5.5, antiCD33-PE, antiCD71-APC, and CD117-PE-Cy7 (all from BD™ Biosciences), the different cell populations were identified according to a sequential and cumulative gating strategy, adapted from the ISHAGE guidelines for stem and progenitor cell analysis by flow cytometry (13), combining specific immunostaining with the analysis of lateral dispersion, or side scatter (SSC), and frontal dispersion, or forward scatter (FSC).

For statistical analysis, numerical variables were summarized by their median and range, and categorical variables by count and relative frequency (percentage). Differences in the distribution of continuous variables were calculated by Mann–Whitney/Kruskal–Wallis tests, while categorical variable comparisons were established by $\chi 2$/Fisher's exact test. A P value <0.05 was considered statistically significant. Analysis was performed with dedicated software (Prism 5, GraphPad Software Inc., San Diego, CA, USA).

3 Results

3.1 Demographic, clinical, and laboratory characteristics at the time of PV diagnosis and leukemic transformation

In both cohorts (post-PV-BP and post-PV-MF-BP), 40% of patients were male (2 out of 5). Median follow-up from PV diagnosis was 83 months (range: 15–190) for post-PV-BP and 118 months (range: 28–301) for post-PV-MF-BP (P=0.6, ns), with a

10.3389/frhem.2024.1356561

mortality rate of 80% (4 out of 5) and 100% (5 out of 5), respectively. Concerning the two APs, post-PV-AP2 died soon after the diagnosis for infectious complications, while post-PV-AP5 was eligible for intensive chemotherapy and underwent allogenic bone marrow transplant (alloHSCT) 10 months after disease progression.

The clinical and laboratory features of PV stage for post-PV-BP and post-PV-MF are summarized in Table 1. Median age at the time of PV diagnosis was similar in the two groups (67 years, range: 49–84 for post-PV-BP and 63 years, range: 42–70 for post-PV-MF-BP). All patients were *JAK2*V617F mutated, while no mutations of *JAK2* exon 12 were found in either group. No differences in hematologic parameters (CBC counts, LDH levels, spleen longitudinal diameter, and history of major thrombotic events) were observed at the time of PV stage in the two groups. BM biopsy revealed a scattered/loose network of reticulin with no/few intersections (fibrosis grade 0/0–1) in all post-PV-BP and in the vast majority (4 out of 5, 80%) of post-PV-MF-BP, with only one patient (1 out of 5, 20%, post-PV-MF-BP2) presenting a fibrosis grade 1. Despite fibrosis grade ≥ 1 at the time of PV diagnosis being associated with reduced myelofibrosis-free survival (14, 15), time to progression to MF of this patient was 96 months, as compared to a median 69 months of the other post-PV-MF cases (range: 11–203 months).

Clinical and laboratory features at the time of evolution to BP are summarized in Table 2. Also at this stage, median age at diagnosis was similar in the two groups (76 years, range: 56–85 for post-PV-BP and 69 years, range: 66–79 for post-PV-MF-BP). Median time to progression from initial PV diagnosis was comparable as well: 7 years (range: 1–14) for post-PV-BP and 8 years (range: 2–24) for post-PV-MF-BP.

At the time of BP transformation, post-PV-MF-BP patients presented with a significantly higher WBC count (median 41.05 × 10^9/L, range: 5.46–58.01) as compared to post-PV-BP patients (median 2.93 × 10^9/L, range: 2.30–39.40, P=0.03) and a significantly larger splenomegaly (median longitudinal diameter by US: 25.5 cm, range: 18–26 vs. 14.0, range: 11.5–20.0, P=0.03). No differences in terms of hemoglobin and hematocrit levels, platelet counts, LDH levels, and percentage of peripheral blood myeloid blasts ($CD34^+$, $CD117^+$, $CD33^+$) were found. Lines of cytoreductive treatment prior to BP are summarized in Table 2: the majority (4 out of 5, 80%) of post-PV-BP underwent only one line of treatment during PV stage, represented by hydroxyurea, while, as expected, post-PV-MF-BP mostly experienced multiple lines of treatment (≥2 in 4 out of 5, 80%), represented by hydroxyurea (all patients), interferon (1 out of 5, 20%), busulfan (1 out of 5, 20%) during PV stage, and the JAK1/2-inhibitor ruxolitinib during the MF stage (3 out of 5, 60%). Of note, history of treatment did not include radiophosphorous, chlorambucil, or pipobroman for both categories.

No differences in OS after diagnosis of leukemic transformation were detected in the two groups (13 months in post-PV-BP vs. 5 months in post-PV-MF-BP, P=0.390).

TABLE 1 Demographic, clinical, and laboratory features at the time of PV diagnosis in post-PV-BP and post-PV-MF-BP.

	post-PV-BP (n=5)	post-PV-MF-BP (n=5)	*P*-value
Age			
Median (range), years	67 (49–84)	63 (42–70)	ns
>67 years, n (%)	3 (60.0)	2 (40.0)	ns
Sex			
Male, n (%)	2 (40.0)	2 (40.0)	ns
Hemoglobin			
Median (range), g/L	169 (155–177)	155 (138–191)	ns
Hematocrit			
Mean (range), %	50.9 (48.9–52.3)	47.6 (42.9–56.0)	ns
WBC count			
Median (range), × 10^9/L	8.14 (6.08–9.06)	12.44 (5.40–17.79)	ns
≥11×10^9/L, n (%)	0 (0.0)	3 (60.0)	ns
≥15×10^9/L, n (%)	0 (0.0)	1 (20.0)	ns
Platelets			
Median (range), × 10^9/L	402 (296–798)	562 (179–742)	ns
LDH			
Mean (range), mU/mL, ×ULN	1.25 (0.65–2.04)	1.30 (0.81–2.23)	ns
Spleen (long. Ø by US)			
Median (range), cm	13.0 (11.0–16.0)	16.7 (10.0–17)	ns
Degree of BM fibrosis			
0/0-1	5 (100.0)	4 (80.0)	ns
1	0 (0.0)	1 (20.0)	
≥ 2	0 (0.0)	0 (0.0)	
***JAK2* mutations**			
Wild type, n (%)	0 (0.0)	0 (0.0)	ns
V617F mutated, n (%)	5 (100.0)	5 (100.0)	
Exon 12 mutated, n (%)	0 (0.0)	0 (0.0)	
Major thrombotic events			
Yes, n (%)	3 (60.0)	3 (60.0)	ns
Erythropoietin (EPO)			
Median (range), U/L*	1.9 (0.9–5.9)	1.4 (0.5–1.4)	ns

*EPO reference lab range: 2.6–19.0 U/L. ns, not significant.

10.3389/frhem.2024.1356561

TABLE 2 Demographic, clinical, and laboratory features at the time of leukemic evolution in post-PV-BP and post-PV-MF-BP.

	post-PV-BP (n=5)	post-PV-MF-BP (n=5)	*P*-value
Age			
Median (range), years	76 (56–85)	69 (66–79)	ns
>67 years, n (%)	4 (80.0)	4 (80.0)	ns
Time to progression from PV			
Median (range), years	7 (1–14)	8 (2–24)	ns
Hemoglobin			
Median (range), g/L	107 (82–108)	82 (76–106)	ns
<100 g/L, n (%)	2 (33.3)	4 (66.7)	ns
Hematocrit			
Mean (range), %	33 (24.4–39.8)	25.2 (22.0–36.0)	ns
WBC count			
Median (range), × 10^9/L	2.93 (2.30–39.40)	41.05 (5.46–58.01)	0.03
>25×10^9/L, n (%)	1 (20.0)	3 (60.0)	ns
Platelets			
Median (range), × 10^9/L	70.0 (55.0–220.0)	59.0 (25.0–127.0)	ns
< 100 x 10^9/L	2 (40.0)	1 (20.0)	ns
LDH			
Mean (range), ×ULN	1.34 (1.16–3.86)	3.64 (1.95–8.9)	ns
Spleen (long. Ø by US)			
Median (range), cm	14.0 (11.5–20.0)	25.5 (18–26)	0.03
Peripheral Blood CD34$^+$ blasts			
Median (range), % Myeloid *(CD33$^+$, CD117$^+$)* Non-myeloid *(CD33$^-$)*	6.5 (1.0–88.0) 0 (0.0)	26.0 (7.5–30.0) 0 (0.0)	ns
>20%, n, %	1 (20.0)	2 (40.0)	ns
AlloHSCT			
Yes, n (%)	1 (20.0)	0 (0.0)	ns
Previous lines of treatment			
1, n (%)	4 (80.0)	1 (20.0)	ns
2, n (%)	1 (20.0)	2 (40.0)	
≥ 3, n (%)	0 (0.0)	2 (40.0)	
Use of ^{32}P, chlorambucil, or pipobroman, n (%)	0 (0.0)	0 (0.0)	
Deaths n %			
Yes, n (%)	4 (80.0)	5 (100.0)	ns

ns, not significant.

3.2 Bone marrow features at the time of leukemic transformation

Bone marrow morphological features and immunophenotype and cytogenetic data during AP/BP for post-PV-BP and post-PV-MF-BP are reported in Table 3.

Post-PV-MF-BP are characterized by a significantly lower cellularity as compared to post-PV-BP (28%, range: 2%–41% vs. 70%, range: 60%–98%, *P*=0.0245; Table 3; Figures 1A–D), with marked reduction of all three hematopoietic lineages (megakaryocytic, erythroid, and myeloid). This is highlighted in Figures 2B, D, F with CD61-, CD71-, and MPO-immunostaining, respectively.

By contrast, post-PV-BP displayed clusters of residual dysplastic erythropoiesis (Figure 2C), megakaryocytic and myeloid hyperplasia with altered topographical dislocation and peculiar dysplastic features (Figures 2A, E), further documented by May-Grunwald Giemsa staining of bone marrow aspirates described in detail below (Figure 3).

In post-PV-MF-BP, indeed, bone marrow architecture is altered by extensive deposition of reticulin fibers, arranged in coarse bundles with numerous intersections, and consequent cellular streaming, compatible with BM fibrosis grade 3 in all subjects, in contrast to post-PV-BP, which, instead, displayed only a mild fibrosis (grade 1 in all cases, *P*=0.008, Table 3; Figures 1E, F), in some cases already present at the time of PV diagnosis (Table 1).

Despite the absolute reduction in overall BM cellularity, BM aspirate immunophenotyping (Table 3) revealed a similar % of myeloid (CD34$^+$, CD117$^+$, and CD33$^+$) blasts, consistent with the CD34 immunostaining of bone marrow biopsies (Figures 1G, H). Flow cytometric analysis of BM cell populations documented a similar % of monocytes/monocyte precursors (CD45^{++}, SCC^{int}), granulocyte/granulocyte precursors (CD45$^+$, SCC^{high}), and nucleated erythroid cells (*CD45$^-$, CD71+*, and *SCC^{low}*).

Finally, in both groups, majority of patients (3 out of 5, 60%) presented a high-risk karyotype.

One of the most striking aspects was that all patients of the post-PV-BP group demonstrated dysplastic features involving all three lineages, while no sign of dysplasia was detectable in the post-PV-MF-BP cohort (*P*=0.008). May-Grunwald-Giemsa staining of BM aspirates from a representative post-PV-BP case (Figures 3A–G) recapitulates these findings. Erythroid dysplasia is clearly documented by the presence of bi-nucleated giant erythroblasts, chromatin bridges, nuclear/cytoplasm maturation asynchrony, and severe nuclear shape abnormalities (yellow arrows in panels A–B, and panel F). Myeloid dysplastic features included neutrophil and granulocyte precursors with nuclear segmentation defects/hyper-segmentation, chromatin clumping, agranular/hypo-granular cytoplasm, and cytoplasmatic vacuoles leading to nuclear dislocation (red arrows in panels A–B and panel E). Hypolobulated/micro-megakaryocytes are as shown in panels C and D, respectively.

10.3389/frhem.2024.1356561

TABLE 3 Bone marrow morphological and cytogenetic features at the time of leukemic evolution in post-PV-BP and post-PV-MF-BP.

	post-PV-BP (n=5)	post-PV-MF-BP (n=5)	*P*-value
BM cellularity			
Median (range), %	70 (60–98)	10 (5–50)	0.025
BM cell population			
Monocytes and monocyte precursors (*CD45*$^{++}$, *SCC*^{int}) Median (range), %	5.0 (3.0–8.0)	4.0 (2.0–15.0)	ns
Granulocytes and granulocyte precursors (*CD45*$^{+}$, *SCC*^{high}) Median (range), %	22.0 (10.0–40.0)	54.0 (36.0–70.0)	ns
CD34^{+} blasts Median (range), % Myeloid (*CD33*$^{+}$, *CD117*$^{+}$) Non-myeloid (*CD33*$^{-}$)	15.0 (8.0–16.0) 0 (0.0)	20.0 (3.0–41.0) 0 (0.0)	ns
Erythroblasts (*CD45*$^{-}$, *CD71*$^{+}$, *SCC*^{low}) Median (range), %	30.0 (20.0–48.0)	33.0 (22.0–44.0)	ns
Degree of BM fibrosis			
0-1	5 (100.0)	0 (0.0)	0.008
≥ 2	0 (0.0)	5 (100.0)	
Dysplasia involving ≥2 lineages			
Yes, n (%)	5 (100.0)	0 (0.0)	0.008
Karyotype			
Normal, n (%)	1 (20.0)	1 (20.0)	ns
Abnormal, n (%)	0 (0.0)	1 (20.0)	
High risk karyotype*, n (%)	3 (60.0)	3 (60.0)	
Not available, n (%)	1 (20.0)	0 (0.0)	

*High-risk karyotype included complex karyotype (defined as ≥ 3 independent abnormalities), −7, inv(3)(q21.3q26.2)/t(3;3)(q21.3;q26.2), i(17)(q10)/-17/abn(17p). ns, not significant.

Panels G and H document BM and PB myeloid blast morphology, respectively, typified by a thin rim of agranular cytoplasm. In panel H, PB dysplastic neutrophils are also detected.

3.3 Molecular features at the time of leukemic transformation

Table 4 summarizes the distribution of pathogenic relevant mutations [category A and B, Functional Analysis through Hidden Markov Models (FATHMM) score >0.90] in the two cohorts (post-PV-BP and post-PV-MF-BP). Nucleotide change, amino-acid substitution, type of mutation (e.g., missense and frameshift), and variant allele frequency (VAF %) are reported for each category A and category B mutation in Supplementary Table 1.

Most commonly mutated genes in the overall AP/BP population (post-PV-BP + post-PV-MF-BP) were *JAK2*V617F, as expected, mutated in 9 out of 10 patients (90%); followed by *ASXL1, DNMT3A, RUNX1*, and *TP53* (4 out of 10, 40%); and *TET2* and *NRAS* (3 out of 10, 30%). Two patients presented *SRSF2* mutation (2 out of 10, 20%), one (1 out of 10, 10%) *IDH1*, and one (1 out of 10, 10%) *IDH2* mutation. All patients carried at least two different mutated genes (median number of mutated genes: 5, range: 2–6), with half of the patients carrying multiple mutations of the same gene, mainly *TET2*. Overall, the median number of mutations was 6 (range: 2–8). In line with the current literature, none of the patients presented *FLT3* and/or *NPM1* mutations, more frequent in *de-novo* AML (4). Of note, post-PV-AP2 lost *JAK2*V617F mutation at the time of leukemic evolution, while post-PV-BP3 also displayed a non-canonical, germline missense *JAK2* mutation [c.3188G>A, p.(Arg1063His), rs77375493], characterized by a G to A substitution at position 3188 listed as probably pathogenetic (category B, score 0.94) in the COSMIC database. Also known as *JAK2*R1063H, this mutation is currently emerging as a functionally relevant mutation in myeloid proliferation, likely cooperating with *JAK2*V617F to favor leukemic transformation (16). Of note, post-PV-BP3 was the only patient for whom NGS data of the PV phase were available and allowed us to compare the mutational status of the chronic vs. blast phase (Supplementary Table 3). As expected, *JAK2*R1063H was already present at the time of PV diagnosis (VAF 54%), together with *JAK2*V617F (VAF 11.8%). Notably, DNMT3A mutation was also detected already at this stage. During leukemic evolution, we registered an increased in the VAF of both mutations (75% for *JAK2*R1063H and 49% for JAK2V617F) and the acquisition of two different *ASXL1* mutations and *CBL* mutation, likely driving clonal evolution.

Comparison of pathogenic relevant mutations of myeloid genes in the two groups showed that *DNMT3A* mutations were present in majority of post-PV-BP (4 out of 5, 80%) and completely absent in the post-PV-MF-BP (*P*=0.048, Table 4). *DNMT3A*, together with *IDH1/2* and *TET2*, segregated along the DNA methylation pathway (5). Notably, all post-PV-BP presented at least one mutation in these genes (with one case, PV-BP2, harboring four different mutations; three in *TET2*; and one in *DNMT3A*). Overall, the frequency of mutations in genes involved in the DNA methylation pathway (*DNMT3A, IDH1/2*, and *TET2*) is significantly higher in the post-PV-BP cohort as compared to post-PV-MF-BP (45% vs. 15%, *P*=0.038).

We also analyzed the frequency of mutations that have been flagged as an SNP in COSMIC database and/or reported as of undetermined significance/benign/likely benign in ClinVar database. All these mutations belong to category C or D and have a low score (<0.5) according to FATHMM and are reported in Supplementary Table 2. No significant enrichment of category C/D mutations was found by comparing post-PV-BP and post-PV-MF-BP. The analysis of category C/D mutations in ClinVar database allowed us to pinpoint recurrent germline variants harbored by all patients (both post-PV-BP and post-PV-MF-BP) located in the

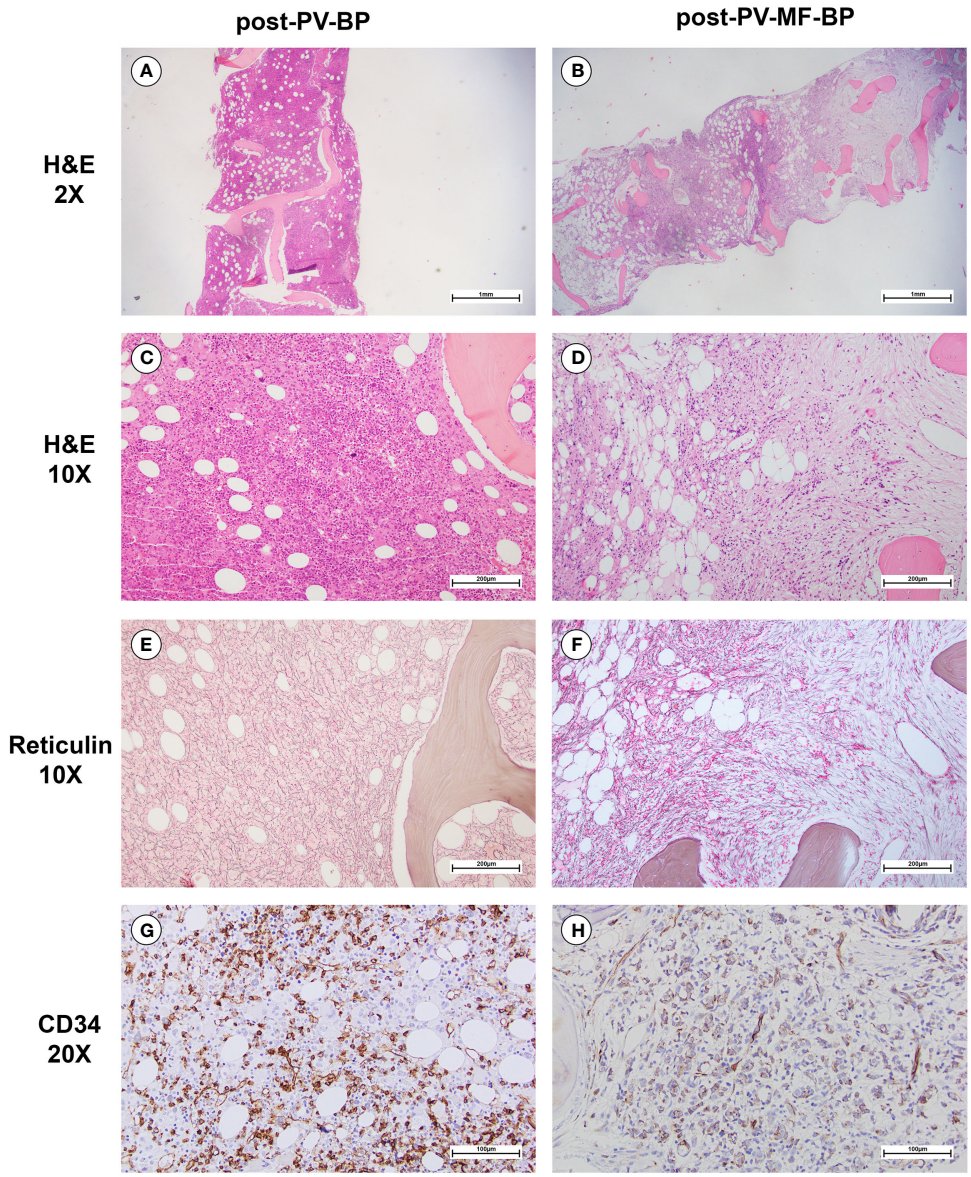

FIGURE 1
Morphological bone marrow features of a representative post-PV-BP and post-PV-MF-BP. **(A–D)** H&E staining showing increased BM cellularity in post-PV-BP **(A, C)**; and dramatically reduced BM cellularity, with cellular streaming in post-PV-MF-BP **(B, D)** (panels **A** and **B**: original magnification 2x, scale bar: 1mm; panels **C** and **D**: original magnification 10x, scale bar: 200µm). **(E)** Reticulin staining of post-PV-BP BM biopsy, showing a loose network of reticulin fibers with few intersections (fibrosis grade 0–1) (original magnification 10x, scale bar: 200 µm). **(F)** Reticulin staining of post-PV-MF-BP BM biopsy, showing a diffuse and dense network of reticulin fibers with extensive intersections (fibrosis grade 3) (original magnification 10x, scale bar: 200 µm). **(G, H)** CD34-immunostaining of post-PV-BP **(G)** and post-PV-MF-BP BM biopsy **(H)** (original magnification 20x, scale bar: 100 µm) showing similar infiltrates of immature myeloid cells.

JAK2 (rs2230722 and rs2230724), *HRAS* (rs12628), *ASXL1* (rs6058694), and *TP53* (rs2454206) genes that have been variably implicated in increased cancer susceptibility (17, 18).

4 Discussion

The natural history of PV encompasses the evolution into post-PV-MF, usually occurring as a late event with reported 10-, 15-, and 20-year incidences of 27.4%, 39.9%, and 61.1%, respectively (19), and the transformation into AP/BP, with incidence estimates of 3%–7% (20). Despite the progress in our understanding of the genetic basis of leukemogenesis (as acknowledged by the 2022 WHO classification), post-PV-AP/BP still lacks a comprehensive characterization and falls into the AML category defined by differentiation (21). Thus, disease-specific clinical, laboratory, and molecular markers are eagerly awaited, to improve diagnosis and define personalized therapeutic approaches.

Depending on the study cohorts, one-third up to approximately one-half of leukemic evolutions occur directly from the PV stage,

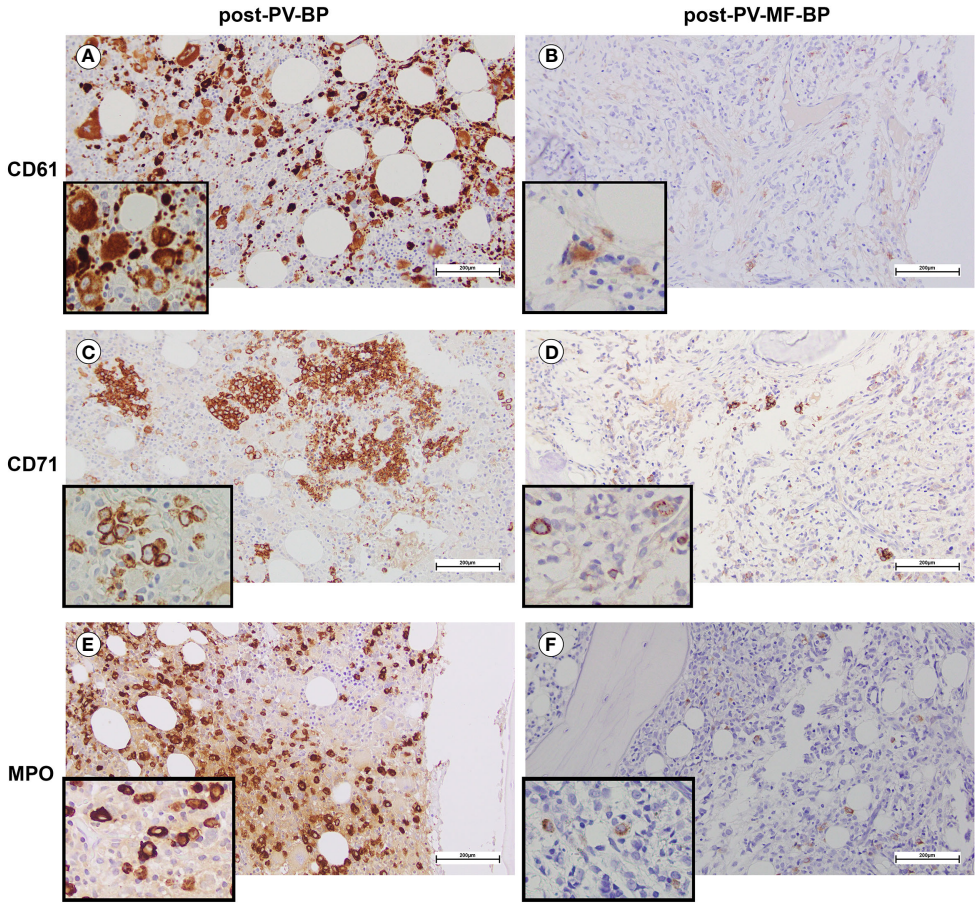

FIGURE 2
BM immunostaining assessing erythroid, megakaryocytic, and myeloid lineages in a representative post-PV-BP and post-PV-MF-BP. **(A, B)** CD61-immunostaining of post-PV-BP **(A)** and post-PV-MF-BP BM biopsy **(B)**. Megakaryocyte hyperplasia with dysplastic features (tight clusters of hypolobulated/mono-nucleated megakaryocytes, insert) is detected in post-PV-BP **(A)** *vs.* megakaryocyte hypoplasia with morphological atypia (hypolobulation, insert) in post-PV-MF-BP **(B)** (original magnification 20×, scale bar: 200 µm; insert 40×). **(C, D)** CD71-immunostaining of a post-PV-BP **(C)** and a post-PV-MF-BP BM biopsy **(D)** showing a marked reduction of the erythroid compartment in post-PV-MF-BP **(D)** *vs.* scattered clusters of residual erythropoiesis with megaloblasts (insert) in post-PV-BP **(C)** (original magnification 20×, scale bar: 200 µm; insert 40×).
(E, F) Myeloperoxidase immunostaining of a post-PV-BP **(E)** and a post-PV-MF-BP **(F)** showing hyperplastic (post-PV-BP) *vs.* reduced (post-PV-MF-BP) myelopoiesis (original magnification 20×, scale bar: 200 µm; insert ×40).

i.e., without a documented overt fibrotic phase. In this study, we targeted the differential morphological, clinical, and molecular features of AP/BP with a direct onset from the PV stage and those of AP/BP arising after the diagnosis of post-PV-MF. To this end, we performed a single-center retrospective descriptive study on 10 post-PV acute myeloid leukemias: 5 post-PV-BP (with two AP), and 5 post-PV-MF-BP.

The two cohorts displayed similar hematologic parameters at the time of PV diagnosis. By contrast, at the time of leukemic evolution, AP/BP directly arising from PV displayed significantly lower leukocyte counts and spleen diameters as compared to those passing through an overt fibrotic phase, likely due to the compensatory extramedullary hematopoiesis that typifies overt fibrotic stages. The most striking differences emerged from BM morphological analysis: all post-PV-BP were characterized by significantly higher cellularity, lower degree of fibrosis, and dysplastic features involving all three lineages, most prominently the erythroid and megakaryocytic compartments. Of note, these aspects were attributable to the intrinsic characteristics of the disease and not to the iatrogenic effects of previous treatment(s), since all 10 patients underwent hydroxyurea for comparable periods (post-PV-BP: median 76 months, range: 16–144 vs. post-PV-MF-BP: 67 months, range: 7–102, P=0.463).

Recent studies have provided valuable insights into the genomic and molecular alterations driving the transition to blast phase in MPNs (7, 8, 17). Mutations in genes such as *TP53, ASXL1*, *IDH1/2*, and *RUNX1* have been identified as key drivers of BP-MPN, contributing to increased genomic instability, resistance to therapy, and clonal evolution (8). Understanding these molecular events is crucial for identifying novel therapeutic targets and designing personalized treatment approaches. NGS analysis of our two cohorts shows that post-PV-BP is significantly enriched in *DNMT3A* mutations, and overall, in mutations of genes that segregate along the DNA methylation pathway (i.e., *TET2* and *IDH1/2*).

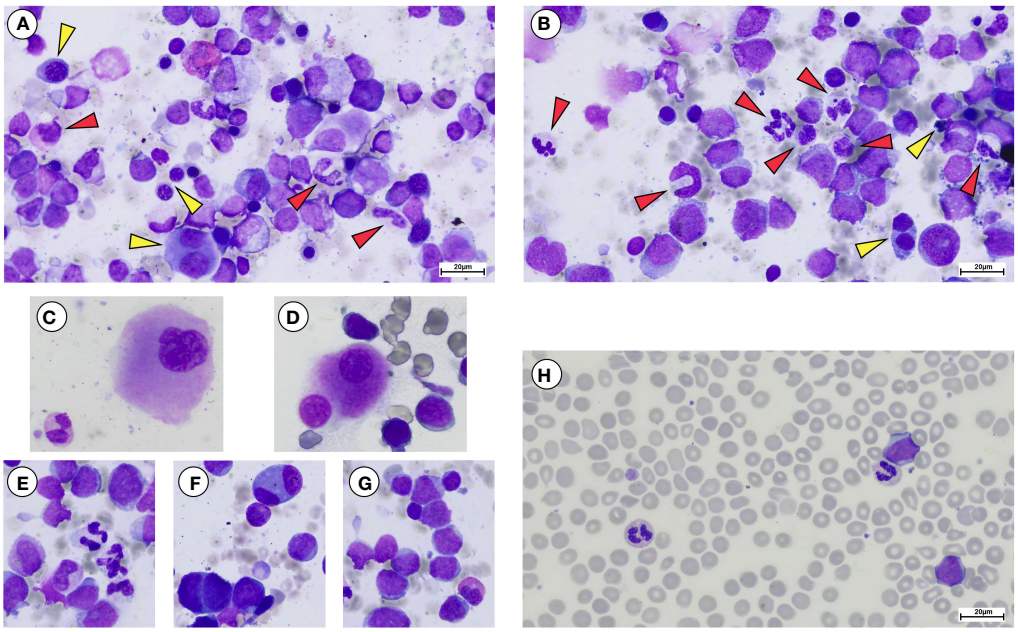

FIGURE 3
May Grunwald-Giemsa staining of bone marrow aspirate and peripheral blood smear of a representative post-PV-BP. **(A–G)** Overview of erythroid myeloid and megakaryocytic lineages showing dysplastic features in bone marrow aspirate. **(A, B)** Erythroid lineage (yellow arrows) showing dysplastic features including presence of chromatin bridges, nuclear/cytoplasmatic maturation asynchrony, bi-nucleated, and giant erythroblasts with nuclear shape abnormalities. **(A, B)** Myeloid lineage (red arrows) showing dysplastic features including nuclear segmentation defects/hypersegmentation, chromatin clumping, hypo-granular cytoplasm, and cytoplasmic vacuoles. **(C, D)** Hypolobulated dysplastic megakaryocytes. **(E)** Dysgranulopoiesis, with myeloid precursors and neutrophils with hypo/agranular cytoplasm, multiple vacuoles causing nuclear dislocation and nuclear segmentation defects. **(F)** Bi-nucleated erythroblasts. **(G)** Myeloid blasts with a thin rim of agranular cytoplasm. A dysplastic hyposegmented eosinophil can also be observed. **(H)** Peripheral blood smear showing myeloid blasts, recapitulating the same characteristic of the BM counterpart. Dysplastic vacuolated neutrophils and a giant platelet can be observed as well (original magnification 40×, scale bar: 20 µm).

DNMT3A and *TET2* are the most frequently identified variants among patients with clonal hematopoiesis of indetermined potential (CHIP) and provide selective advantage that foster clonal expansion and myeloid skewing. Both genes are more frequently mutated in MDS and MDS/MPN as compared to PV (22) and both increase in frequency in secondary AML (either post-MDS or post-MPN) (23). However, while *DNMT3A* mutations are generally present in early-stage disease, *TET2* mutation can occur either before or after the acquisition of *JAK2*V617F mutation, leading to a biclonal disease or to a competitive advantage driving clonal dominance (24). In our cohort, we were able to retrieve NGS data at the time of PV diagnosis for one patient (post-PV-BP3), demonstrating that *DNMT3A* and *JAK2* mutations were already present in the chronic stage. Based on the accumulating evidence on the molecular hits during the history of these disorders, we can speculate that the acquisition of *DNMT3A* mutation might occur as an early genetic event that might play a role in the dysplastic phenotype that typifies post-PV-BP. Indeed, clonality studies are necessary to answer this question and to assess whether the pre-leukemic clones in the two examined patient groups are independent or not from the clones driving chronic phase PV or post-PV-MF.

Our analysis also detected a non-canonical mutation of *JAK2*, namely, *JAK2*R1063H. A growing body of literature is highlighting the potential clinical significance of this germline variant in the MPN setting. Indeed, *JAK2*R1063H weakly hyperactivates JAK2/STAT5 signaling as compared to the acquired somatic V617F, but likely cooperates with another germline variant, *JAK2*E846D, in hereditary erythrocytosis (25) and with *JAK2*V617F itself in MPNs, favoring a more aggressive disease phenotype with significantly higher neutrophil counts and enrichment in thrombotic events (26). A potential pro-thrombotic role of this variant is further supported by a whole-exome sequencing study conducted in 22 young ischemic stroke patients with familial clustering of stroke, in which *JAK2*R1063H was detected in a proband with embolic stroke of undetermined source and prothrombotic status (27). Finally, in a subsequent next-generation sequencing study on 2154 MPN, MPN-BP, and AML patients, *JAK2*R1063H was predicted to have a functional consequence on JAK2 by three distinct predictive algorithms and was associated with an increased risk of leukemic transformation when combined with canonical *JAK2* mutation (16).

NGS analysis also allowed information retrieval on genetic variations that have been flagged as an SNP and/or reported as of undetermined significance/benign/likely benign. Although no differences were found among post-PV-BP and post-PV-MF-BP, our analysis shed light onto germline variants of potential interest in MPN-BP, such as *JAK2* (rs2230722 and rs2230724), *HRAS* (rs12628), *ASXL1* (rs6058694), and *TP53* (rs2454206).

10.3389/frhem.2024.1356561

TABLE 4 Distribution of pathogenetically relevant (category A and B) mutations in cohort 1 (post-PV-BP1-5) and in cohort 2 (post-PV-MF-BP1-5).

	post-PV-BP					post-PV-MF-BP				
	post-PV-BP1	post-PV-AP2	post-PV-BP3	post-PV-BP4	post-PV-AP5	post-PV-MF-BP1	post-PV-MF-BP2	post-PV-MF-BP3	post-PV-MF-BP4	post-PV-MF-BP5
ABL1										
ASXL1			2							
BRAF										
CALR										
CBL										
CEBPA										
CSF3R										
DNMT3A										
ETV6										
EZH2										
FLT3										
HRAS										
IDH1										
IDH2										
JAK2			2							
KIT										
KRAS										
MPL										
NPM1										
NRAS										
PTPN11				3						
RUNX1										
SETBP1										
SF3B1										
SRSF2										
TET2		3							2	
TP53										2
U2AF1										
WT1										
ZRSR2										
Total no. of mutated genes	6	4	4	6	2	5	2	2	4	5
Total no. of mutations	6	6	6	8	2	5	2	5	5	6

All genes analyzed with the Myeloid Solutions Panel (SOPHiA Genetics) are shown. Colored boxes indicate the presence of category A and B mutations. In case of the presence of >1 category A and B mutations for a specific gene, the number of mutations is indicated in the respective boxes. The total number of mutated genes and total number of mutations for each patient are reported in the last two rows.

HRAS rs12628, originally described by Taparowsky et al. (28), was shown to be associated with increased risk of oral carcinoma, colon, gastric and bladder cancer, and cutaneous melanoma (18, 29–31). This genetic variant has also been associated with syndromic congenital disorders, such as Noonan syndrome, Noonan-related syndrome, and Costello Syndrome (32). To the best of our knowledge, no data are currently available on the contribution of this SNP to hematologic malignancies. *JAK2* rs2230722, located in exon 6, and *JAK2* rs2230724, present in exon 19 have already been described in MPNs (17), with the latter being associated with the progression to BP, especially in individuals older than 45 years old (33) and therefore suggested as a potential genetic marker of leukemic progression in MPNs. *ASXL1* rs6058694 has been reported in AML (34) and in a case report of triple-negative ET unresponsive to therapy (35). Additionally, *TP53* rs2454206 has been extensively investigated as a germline predisposition factor for cancer. Despite conflicting data, this SNP may increase the risk of colorectal cancer (36), chronic lymphocytic leukemia (37), and acute myeloid leukemia with adverse molecular and cytogenetic risk (38).

With all the limits of the small number of patients studied and the descriptive intent, this is the first report formally describing recurrent morphological, clinical, and hematological stigmata that differentiate BPs that arise directly from PV from those occurring after post-PV-MF. This peculiar phenotype is consistent with the molecular signature of the disease, typified by mutations of genes involved in the DNA methylation pathways, occurring with a high frequency in MDS and MDS/MPN, leading us to speculate that BP occurring directly from the "florid" phase might be characterized by a distinct physiopathological mechanism.

Further studies in larger cohorts are warranted to translate these observations into robust evidence that may guide diagnosis and advise targeted therapeutic choices, like, for instance, hypomethylating agents.

Data availability statement

The raw data supporting the conclusions of this article will be made available by the authors, without undue reservation.

Ethics statement

The studies involving humans were approved by Area Vasta Emilia Nord Ethical Commitee (prot. 6923, 17/02/2020). The studies were conducted in accordance with the local legislation and institutional requirements. The participants provided their written informed consent to participate in this study.

Author contributions

LPe: Investigation, Writing – original draft, Data curation. GP: Data curation, Investigation, Methodology, Writing – original draft. SC: Methodology, Investigation, Writing – original draft. CM: Methodology, Writing – review & editing. EuM: Methodology, Writing – review & editing. LPa: Writing – review & editing, Investigation. MG: Writing – review & editing, Investigation. GR: Writing – review & editing, Supervision. MV: Conceptualization, Supervision, Writing – review & editing. CC: Conceptualization, Data curation, Writing – original draft, Supervision, Writing – review & editing. ElM: Conceptualization, Data curation, Funding acquisition, Writing – original draft, Supervision, Writing – review & editing.

Funding

The author(s) declare financial support was received for the research, authorship, and/or publication of this article. Fondi Locali per la Ricerca 2023, Quota Prodotti di Ricerca, Parma University to ElM and CC.

Conflict of interest

The authors declare that the research was conducted in the absence of any commercial or financial relationships that could be construed as a potential conflict of interest.

The author(s) declared that they were an editorial board member of Frontiers, at the time of submission. This had no impact on the peer review process and the final decision.

Publisher's note

Supplementary material

The Supplementary Material for this article can be found online at: https://www.frontiersin.org/articles/10.3389/frhem.2024.1356561/full#supplementary-material

References

1. Scott LM, Tong W, Levine RL, Scott MA, Beer PA, Stratton MR, et al. JAK2 exon 12 mutations in polycythemia vera and idiopathic erythrocytosis. *N Engl J Med*. (2007) 356:459–68. doi: 10.1056/NEJMoa065202

2. Tefferi A, Barbui T. Polycythemia vera: 2024 update on diagnosis, risk-stratification, and management. *Am J Hematol*. (2023) 98:1465–87. doi: 10.1002/ajh.27002

3. Tefferi A, Mudireddy M, Mannelli F, Begna KH, Patnaik MM, Hanson CA, et al. Blast phase myeloproliferative neoplasm: Mayo-AGIMM study of 410 patients from two separate cohorts. *Leukemia*. (2018) 32:1200–10. doi: 10.1038/s41375-018-0019-y

4. Ajufo HO, Waksal JA, Mascarenhas JO, Rampal RK. Treating accelerated and blast phase myeloproliferative neoplasms: progress and challenges. *Ther Adv Hematol*. (2023) 14:20406207231177282. doi: 10.1177/20406207231177282

5. Patel AA, Odenike O. SOHO state of the art updates and next questions | Accelerated phase of MPN: what it is and what to do about it. *Clin Lymphoma Myeloma Leuk*. (2023) 23:303–9. doi: 10.1016/j.clml.2023.01.011

6. Tefferi A, Guglielmelli P, Lasho TL, Coltro G, Finke CM, Loscocco GG, et al. Mutation-enhanced international prognostic systems for essential thrombocythaemia and polycythaemia vera. *Br J Haematol*. (2020) 189:291–302. doi: 10.1111/bjh.16380

7. Mannelli F. Acute myeloid leukemia evolving from myeloproliferative neoplasms: many sides of a challenging disease. *J Clin Med*. (2021) 10:436. doi: 10.3390/jcm10030436

8. Grabek J, Straube J, Bywater M, Lane SW. MPN: the molecular drivers of disease initiation, progression and transformation and their effect on treatment. *Cells*. (2020) 9:1901. doi: 10.3390/cells9081901

9. McNamara CJ, Panzarella T, Kennedy JA, Arruda A, Claudio JO, Daher-Reyes G, et al. The mutational landscape of accelerated- and blast-phase myeloproliferative neoplasms impacts patient outcomes. *Blood Adv*. (2018) 2:2658–71. doi: 10.1182/bloodadvances.2018021469

10. Tefferi A, Cervantes F, Mesa R, Passamonti F, Verstovsek S, Vannucchi AM, et al. Revised response criteria for myelofibrosis: International Working Group-Myeloproliferative Neoplasms Research and Treatment (IWG-MRT) and European LeukemiaNet (ELN) consensus report. *Blood*. (2013) 122:1395–8. doi: 10.1182/blood-2013-03-488098

11. Arber DA, Orazi A, Hasserjian R, Thiele J, Borowitz MJ, Le Beau MM, et al. The 2016 revision to the World Health Organization classification of myeloid neoplasms and acute leukemia. *Blood*. (2016) 128:462–3. doi: 10.1182/blood-2016-06-721662

12. Thiele J, Kvasnicka HM, Facchetti F, Franco V, van der Walt J, Orazi A. European consensus on grading bone marrow fibrosis and assessment of cellularity. *Haematologica*. (2005) 90:1128–32.

13. Sutherland DR, Anderson L, Keeney M, Nayar R, Chin-Yee I. The ISHAGE guidelines for CD34+ cell determination by flow cytometry. International Society of Hematotherapy and Graft Engineering. *J Hematother*. (1996) 5:213–26. doi: 10.1089/scd.1.1996.5.213

14. Barbui T, Thiele J, Passamonti F, Rumi E, Boveri E, Randi ML, et al. Initial bone marrow reticulin fibrosis in polycythemia vera exerts an impact on clinical outcome. *Blood*. (2012) 119:2239–41. doi: 10.1182/blood-2011-11-393819

15. Barraco D, Cerquozzi S, Hanson CA, Ketterling RP, Pardanani A, Gangat N, et al. Prognostic impact of bone marrow fibrosis in polycythemia vera: validation of the IWG-MRT study and additional observations. *Blood Cancer J*. (2017) 7:e538. doi: 10.1038/bcj.2017.17

16. Benton CB, Boddu PC, DiNardo CD, Bose P, Wang F, Assi R, et al. Janus kinase 2 variants associated with the transformation of myeloproliferative neoplasms into acute myeloid leukemia. *Cancer*. (2019) 125:1855–66. doi: 10.1002/cncr.31986

17. Torres DG, Barbosa Alves EV, Araújo de Sousa M, Laranjeira WH, Paes J, Alves E, et al. Molecular landscape of the JAK2 gene in chronic myeloproliferative neoplasm patients from the state of Amazonas, Brazil. *BioMed Rep*. (2023) 19:98. doi: 10.3892/br.2023.1680

18. Tomei S, Adams S, Uccellini L, Bedognetti D, De Giorgi V, Erdenebileg N, et al. Association between HRAS rs12628 and rs112587690 polymorphisms with the risk of melanoma in the North American population. *Med Oncol*. (2012) 29:3456–61. doi: 10.1007/s12032-012-0255-3

19. Bai J, Ai L, Zhang L, Yang FC, Zhou Y, Xue Y. Incidence and risk factors for myelofibrotic transformation among 272 Chinese patients with JAK2-mutated polycythemia vera. *Am J Hematol*. (2015) 90:1116–21. doi: 10.1002/ajh.24191

20. Tefferi A, Alkhateeb H, Gangat N. Blast phase myeloproliferative neoplasm: contemporary review and 2024 treatment algorithm. *Blood Cancer J*. (2023) 13:108. doi: 10.1038/s41408-023-00878-8

21. Khoury JD, Solary E, Abla O, Akkari Y, Alaggio R, Apperley JF, et al. The 5th edition of the World Health Organization classification of haematolymphoid tumours: myeloid and histiocytic/dendritic neoplasms. *Leukemia*. (2022) 36:1703–19. doi: 10.1038/s41375-022-01613-1

22. Stegelmann F, Bullinger L, Schlenk RF, Paschka P, Griesshammer M, Blersch C, et al. DNMT3A mutations in myeloproliferative neoplasms. *Leukemia*. (2011) 25:1217–9. doi: 10.1038/leu.2011.77

23. Fried I, Bodner C, Pichler MM, Lind K, Beham-Schmid C, Quehenberger F, et al. Frequency, onset and clinical impact of somatic DNMT3A mutations in therapy-related and secondary acute myeloid leukemia. *Haematologica*. (2012) 97:246–50. doi: 10.3324/haematol.2011.051581

24. Vainchenker W, Kralovics R. Genetic basis and molecular pathophysiology of classical myeloproliferative neoplasms. *Blood*. (2017) 129:667–79. doi: 10.1182/blood-2016-10-695940

25. Kapralova K, Horvathova M, Pecquet C, Fialova Kucerova J, Pospisilova D, Leroy E, et al. Cooperation of germ line JAK2 mutations E846D and R1063H in hereditary erythrocytosis with megakaryocytic atypia. *Blood*. (2016) 128:1418–23. doi: 10.1182/blood-2016-02-698951

26. Mambet C, Babosova O, Defour JP, Leroy E, Necula L, Stanca O, et al. Cooccurring JAK2 V617F and R1063H mutations increase JAK2 signaling and neutrophilia in myeloproliferative neoplasms. *Blood*. (2018) 132:2695–9. doi: 10.1182/blood-2018-04-843060

27. Ilinca A, Martinez-Majander N, Samuelsson S, Piccinelli P, Truvé K, Cole J, et al. Whole-exome sequencing in 22 young ischemic stroke patients with familial clustering of stroke. *Stroke*. (2020) 51:1056–63. doi: 10.1161/STROKEAHA.119.027474

28. Taparowsky E, Suard Y, Fasano O, Shimizu K, Goldfarb M, Wigler M. Activation of the T24 bladder carcinoma transforming gene is linked to a single amino acid change. *Nature*. (1982) 300:762–5. doi: 10.1038/300762a0

29. Johne A, Roots I, Brockmöller J. A single nucleotide polymorphism in the human H-ras proto-oncogene determines the risk of urinary bladder cancer. *Cancer Epidemiol Biomarkers Prev*. (2003) 12:68–70.

30. Catela Ivkovic T, Loncar B, Spaventi R, Kapitanovic S. Association of H-ras polymorphisms and susceptibility to sporadic colon cancer. *Int J Oncol*. (2009) 35:1169–73. doi: 10.3892/ijo_00000433

31. Pandith AA, Shah ZA, Khan NP, Baba KM, Wani MS, Siddiqi MA. HRAS T81C polymorphism modulates risk of urinary bladder cancer and predicts advanced tumors in ethnic Kashmiri population. *Urol Oncol*. (2013) 31:487–92. doi: 10.1016/j.urolonc.2011.03.004

32. Sol-Church K, Stabley DL, Nicholson L, Gonzalez IL, Gripp KW. Paternal bias in parental origin of HRAS mutations in Costello syndrome. *Hum Mutat*. (2006) 27:736–41. doi: 10.1002/humu.20381

33. Zhong Y, Wu J, Ma R, Cao H, Wang Z, Ding J, et al. Association of Janus kinase 2 (JAK2) polymorphisms with acute leukemia susceptibility. *Int J Lab Hematol*. (2012) 34:248–53. doi: 10.1111/j.1751-553X.2011.01386.x

34. Pellegrino M, Sciambi A, Treusch S, Durruthy-Durruthy R, Gokhale K, Jacob J, et al. High-throughput single-cell DNA sequencing of acute myeloid leukemia tumors with droplet microfluidics. *Genome Res*. (2018) 28:1345–52. doi: 10.1101/gr.232272.117

35. Zaidi U, Shahid S, Fatima N, Ahmed S, Sufaida G, Nadeem M, et al. Genomic profile of a patient with triple negative essential thrombocythemia, unresponsive to therapy: A case report and literature review. *J Adv Res*. (2017) 8:375–8. doi: 10.1016/j.jare.2017.04.001

36. Elshazli RM, Toraih EA, Elgaml A, Kandil E, Fawzy MS. Genetic polymorphisms of TP53 (rs1042522) and MDM2 (rs2279744) and colorectal cancer risk: An updated meta-analysis based on 59 case-control studies. *Gene*. (2020) 734:144391. doi: 10.1016/j.gene.2020.144391

37. Ounalli A, Moumni I, Mechaal A, Chakroun A, Barmat M, Rhim REE, et al. TP53 Gene 72 Arg/Pro (rs1042522) single nucleotide polymorphism increases the risk and the severity of chronic lymphocytic leukemia. *Front Oncol*. (2023) 13:1272876. doi: 10.3389/fonc.2023.1272876

38. Tripon F, Iancu M, Trifa A, Crauciuc GA, Boglis A, Balla B, et al. Association Analysis of TP53 rs1042522, MDM2 rs2279744, rs3730485, MDM4 rs4245739 Variants and Acute Myeloid Leukemia Susceptibility, Risk Stratification Scores, and Clinical Features: An Exploratory Study. *J Clin Med*. (2020) 9:1672. doi: 10.3390/jcm9061672